Journal of Statistical Physics, Vol. 64, Nos. 5/6, 1991

Localized Bifurcations and Defect Instabilities in the Convection of a Nematic Liquid Crystal

A. Joets[1] **and R. Ribotta**[1]

The stationary and the time-dependent homogeneous ordered states in convection may both become unstable against localized perturbations. Defects are then created and they may contribute to the disorganization of the homogeneous state. We present an experimental study of defects in some homogeneous stationary structures as well as in the traveling-wave states of convection of a nematic liquid crystal. We show that the core of the defects is a germ of the unstable state and it can become unstable under the external stress. Then, either fully homogeneous states with the symmetry of the core, or complex disordered states can develop from the local instability of defects in processes quite similar to displacive transitions in solids. Some of the main features are qualitatively similar to numerical simulations of an appropriate Landau–Ginzburg equation.

KEY WORDS: Convection; nematic liquid crystal; localized bifurcations; defects.

1. INTRODUCTION

Nonlinear systems subjected to an increasing external stress may undergo a series of bifurcations to ordered stable states before reaching a full disordered state (space-time chaos). These ordered states may be stationary or time-dependent or both. Usually, one would consider only the homogeneous states, i.e., those which are characterized by an amplitude independent of space. However, it is very often found experimentally that under some circumstances, these states may become unstable under localized perturbations.[1,2] One of the consequences, as will be shown hereafter, is the nucleation of defects in the ordered state. The defects may

[1] Laboratoire de Physique des Solides, Université de Paris-Sud, 91405 Orsay Cedex, France.

0022-4715/91/0900-0981$06.50/0

in turn become unstable under the applied stress and develop in space a localized state with a lower symmetry. As the stress is kept increasing, a new homogeneous stable state can then be germinated and invade the whole space.

We shall here study experimentally the quasistationary states as well as the ordered structures represented by 1D traveling waves.[3] The similarity between those two cases that are commonly found in the convection of a nematic liquid crystal is shown to arise from the symmetry of the considered states. The dynamics of the evolution of the defects under applied stresses has also a striking counterpart in the thermodynamic phase transitions of solids. Novel numerical simulations of a Landau–Ginzburg model shall be used for showing that defects are solutions and for qualitative comparison.

2. HOMOGENEOUS STRUCTURES AND DEFECTS

2.1. The Experiment

The physical model is given by the convective instabilities developed in a nematic liquid crystal subjected to an AC electric field in the so-called "conduction regime."[4] The geometry is the usual one for nematics with negative dielectric anisotropy: the molecules are in the planar (homogeneous) alignment, i.e., parallel to the glass plates between which the fluid is sandwiched. The electric field is applied across the layer of typical thickness ranging from 10 to 50 μm. We use either MBBA or Merck Phase IV.

Above a well-defined voltage threshold V_{th} the layer becomes unstable against a convective state characterized by a spatial periodicity along the molecular direction (say **x**). The structures are recorded through a polarizing microscope and analyzed using computer-controlled digital processing. For the one-dimensional traveling rolls we proceed as follows: in each picture we record the intensity of the transmitted light along one line parallel to **x**. So, at a given time, a wave is recorded as a periodic array of white dots (the crests of maximum intensity) separated by black spaces (the wave wells). The operation is repeated at equal time intervals and the successive recordings are plotted on top of each other in order to compose a 2D image which is the space-time $\{x, t\}$ representation of the wave. A progressive wave will then appear as a set of parallel oblique lines tilted by an angle θ onto the vertical axis t, which gives a direct measurement of the phase velocity $v = \tan\theta$. It is found that the structure propagates along **x** with a uniform velocity increasing with the inverse of the sample thickness and more sharply in the higher-frequency range.[3] Typically, velocities v up

to some fraction of a wavelength $\lambda = 2\pi/q$ per second can be recorded. The smallest values are close to 10^{-4} λ/sec in the middle of the frequency range and for thickness of about 50 μm. There the structures can be considered as stationary.

In order to study 1D waves, we operate at high frequencies or with small-thickness samples. Then, we prepare the experiment so that the extension of the rolls along their axis **y** is of the order of their diameter. This is done using narrow electrodes 50 μm wide along **y** and 2 cm along **x**. Very close to threshold the traveling wave keeps stable and uniform, but as the control parameter, here the voltage V, is increased to reach values such that $\varepsilon = (V^2 - V_{th}^2)/V_{th}^2 \simeq 10^{-2}$ to 10^{-1}, it becomes unstable against localized instabilities from which defects usually arise.

2.2. The Stability Diagram

The frequency of the applied AC voltage being a secondary control parameter, a stability diagram can be obtained by measuring the voltage threshold for a bifurcation, at any frequency. Two typical routes to the chaotic (the lowest symmetry) state are found, depending on the rate of application of the voltage.[5,6]

(a) If, typically, $\Delta V/\Delta t < 20$ mV/min, a series of well-defined bifurcations occurs as V increases until the full chaotic state (Dynamic Scattering Mode[4]). As V increases, the stable states are, in order: the Normal Rolls, the Oblique Rolls (or zigzag), the Skew Varicose, and the Bimodal (Fig. 1).

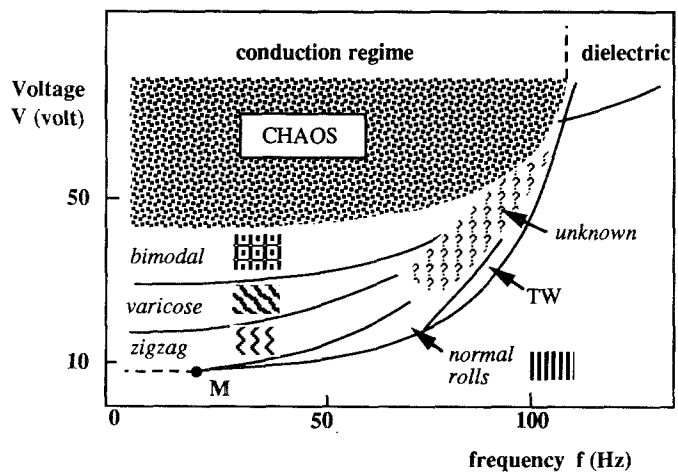

Fig. 1. Bifurcation lines in the voltage–frequency space. As V increases slowly, the space-time chaos is reached through a series of bifurcations ($d = 50$ μm).

The flows associated with each state are studied by tracing small glass spheres, 3–5 μm in diameter, immersed in the fluid.[6–8]

The sequence of stable bifurcations then corresponds to the evolution from a pure "monomode" of rotation around the roll axis in the Normal Rolls, to a double mode of two orthogonal rotations around the x and y axes in the Bimodal. The Bimodal is the last ordered state before the chaos starts developing. The key mechanism in the flow evolution is the pinching of the Varicose, which produces locally a rotation of the vorticity by almost $\pi/2$, and induces stagnation points in the flow.[9]

It is worth noting that here in this anisotropic fluid, the Oblique Rolls and the Varicose are *stable* stationary states, as opposed to the case of isotropic experiments (Rayleigh–Bénard), where they are transient states.[10]

(b) If, at the same frequency, the voltage is rather increased at a higher rate, then very soon beyond the first bifurcation to the Normal Rolls a complex state is developed (Fig. 2). For instance, if $\Delta V/\Delta t \simeq$ 100 mV/sec right above the first threshold, defects are spontaneously created in the whole sample with a low density at start. The mean separation length between defects is of order 10λ. Simultaneously, time dependence occurs as a slow lateral motion of rolls inside domains that are decorrelated in time. The domains are separated by defects. The defects as well as the structure move in an apparent random mode of motion.

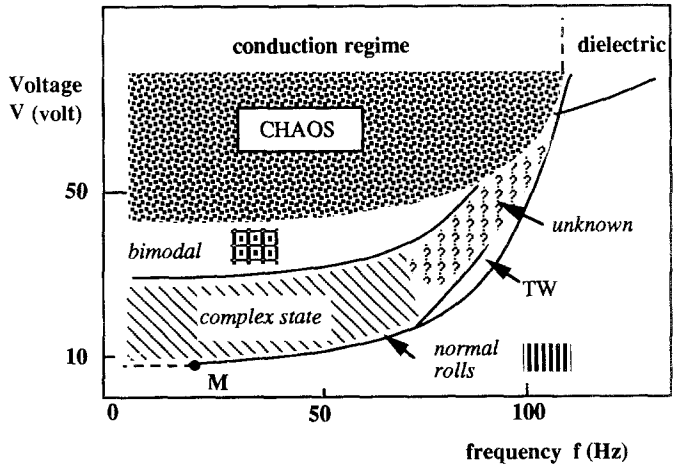

Fig. 2. The transition from the Normal Rolls to the chaotic state is mediated by a complex state involving defects and a time-dependent state, as the voltage is rapidly increased ($d = 50$ μm).

Increasing further the voltage increases the defect density as well as their average velocity. There, the motion appears as due to an oscillation of the amplitude that develops inside the domains[5] as an exchange between the two symmetrical states of Oblique Rolls.[11] The OR states are then coupled by a Hopf-like bifurcation. Simultaneously, the defects extend their core normally to the roll axis on lines which we shall name "dissociation lines" (see Section 2.3), and which appear as bright streaks on a dark background (Figs. 3 and 12). This second route to the Bimodal and the chaotic states indicates that the defects are involved in a transient process, implying localized deformations of the structure. This is the fastest way by which the homogeneous Bimodal state can be obtained *directly*[5] from the Normal Rolls (Fig. 2) and in fact, this complex state was quite commonly observed[12] right above the threshold of the so-called "Williams Domains" instead of the Oblique Rolls and the Varicose.

We shall show later that such a process can be in a large part understood after the study of the stability of a defect under applied stress. In addition, numerical simulations are made to show that defects may arise as natural solutions of the problem.

2.3. The Model for Stationary States of Convective Rolls

A 2D homogeneous structure of rolls (here the Normal Rolls) is described by a local quantity, for instance, the vertical velocity component:

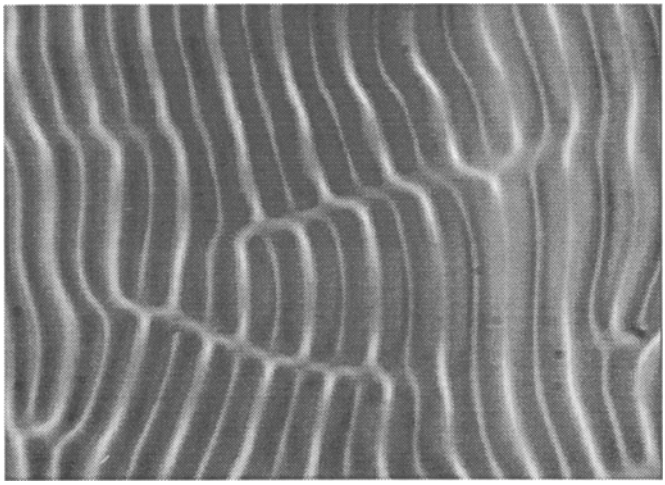

Fig. 3. The complex state developed under rapid increase of the voltage ($f = 50$ Hz, $V = 12.6$ V, $d = 50$ μm).

$u_z(x, y, t) \sim A(X, Y, T) \exp i(k_0 x) + \text{c.c}$, where, to account for the slow variations of the amplitude, the variables x, y, and t have been rescaled so that $X = \sqrt{\varepsilon}\, x$, $Y = \sqrt{\varepsilon}\, y$, $T = \varepsilon t$, where ε is the relative increase of the stress, and $A = A_0 \exp i\varphi$. The structure is homogeneous and stable if $A_0 = \text{const}$. The amplitude A is the envelope of $u(x, t)$ and is a solution to a time-dependent nonlinear equation of the Landau–Ginzburg type[13] which can in principle be derived[14] from the basic microscopic equations for the DGP model[4]:

$$\partial A/\partial t = \mu A + \Delta A - \beta |A|^2 A$$

where t has again be rescaled.

A uniform periodic structure of rolls is characterized by $\varphi = \text{const}$ and by a wavevector $\mathbf{k}_0$ along $\mathbf{x}$ such that $k_0 = \text{grad}\, \Phi$, where $\Phi = k_0 x + \varphi$. If the order parameter is now allowed to vary slowly in space, then $\varphi = \varphi(x, y, t)$. Inside an almost homogeneous structure, where small distortions in the ordering appear, the perfect ordering can in principle be recovered by any small deformation, and the total phase variation along any oriented closed contour C in the plane is zero, $\oint_C (\text{grad}\, \Phi) \cdot ds = 0$. The variable $A(x, y, t)$ can be considered as an order parameter which characterizes the state, as in phase transitions. Its value is zero in the basic unstable state, and finite in the bifurcated state. The Normal Rolls are described by $u_{\text{NR}} \sim \text{Re}\{A_0 \exp i(k_x x)\}$, the Oblique Rolls by $u_{\text{OR}} \sim \text{Re}\{A_1 \exp i(k_x x \pm k_y y)\}$, and the homogeneous structures of lower symmetry can be considered as a superposition of the higher symmetry states that break the translational invariance along $\mathbf{y}$, i.e., the Oblique Rolls. So, the Skew Varicose is the superposition of two symmetrical Oblique Rolls with different amplitudes:

$$u_{\text{SV}} \sim \text{Re}\{A_1 \exp i(k_x x + k_y y) + \eta A_1 \exp i(k_x x - k_y y)\}$$

where $\eta < 1$, and the Bimodal is obtained in the same way, but with $\eta = 1$.

2.4. The Model for the One-Dimensional Traveling Rolls

The traveling-wave convective state found[3,5] mainly at high frequencies for thick samples $d > 30\ \mu\text{m}$ (see Fig. 1) or at any frequency for thin ($< 20\ \mu\text{m}$) samples is a simple example of a nonlinear wave.[16] Waves are ordered structures of space-time and they propagate in either the $-\mathbf{x}$ or $\mathbf{x}$ direction. A local quantity is expressed as

$$u(x, t) = \text{Re}\{A(X, T) \exp i(kx - \omega t) + B(X, T) \exp i(kx + \omega t)\} \cdot f(z)$$

The system is then described by two coupled complex Landau–Ginzburg

(CLG) amplitude equations[17] which, after appropriate rescaling and keeping the same notations for the variables, read

$$\frac{\partial A}{\partial t} + c_g \frac{\partial A}{\partial x} = \mu A + (1 + i\alpha) \frac{\partial^2 A}{\partial x^2} - (1 + i\beta) |A|^2 A - (\gamma + i\delta) |B|^2 A$$

$$\frac{\partial B}{\partial t} - c_g \frac{\partial B}{\partial x} = \mu A + (1 + i\alpha) \frac{\partial^2 B}{\partial x^2} - (1 + i\beta) |B|^2 B - (\gamma + i\delta) |A|^2 B$$

The most unstable mode grows with a rate determined by (μA) and its amplitude is limited by the saturation $(|A|^2 A)$. The second term is for the diffusion by $(\partial^2 A/\partial x^2)$ and for the dispersion of the wave by $(i\alpha\, \partial^2 A/\partial x^2)$. The complex term, $i\beta |A|^2 A$, expresses the coupling between the frequency and the amplitude, and the last term is for the coupling between the left and right waves. The coefficient c_g is the group velocity.

The solutions are:

(i) A uniform right-going wave, $|A| \neq 0$ with $|B| = 0$; or left-going: $|B| \neq 0$, $|A| = 0$.

(ii) A standing wave (SW), where A and B are coupled, $|A| = |B|$.

The progressive waves are unstable against standing waves when $|\gamma| < 1$. They also may undergo phase instabilities (of the Benjamin–Feir type) when $\gamma > 1$, if the condition $(1 + \alpha\beta) < 0$ is fulfilled.[13,18]

However, we shall be concerned in the following with the more complex case of nonhomogeneous perturbations (i.e., localized ones), which usually trigger instabilities involving both the phase and the amplitude. It is known that nonlinear waves may develop localized states such as solitons,[18] or more complex states responsible for the wave breaking, such as shocks.[16] As we shall see, defects are created after shocks are produced by localized modulational instabilities.

2.5. Symmetries in the 2D Homogeneous Stationary and Time-Dependent States

The nature of the possible defects is determined by the symmetries that are broken by the bifurcated state[19] and there exists a similarity either between the structures or between their defects in the stationary and in the time-dependent states. The phase of the Oblique Rolls is $(k_x x \pm k_y y)$, and it is $(k_x x \pm \omega t)$ in a progressive wave. Then, ωt and $k_y y$ play the same role, reflecting the symmetries $\theta \rightleftharpoons -\theta$, where $\theta = \arctan(k_y/k_x)$, and $v \rightleftharpoons -v$, where v is the phase velocity $v = \omega/k_x$. In addition, from these basic states, one can construct by superposition the lower symmetry ones,

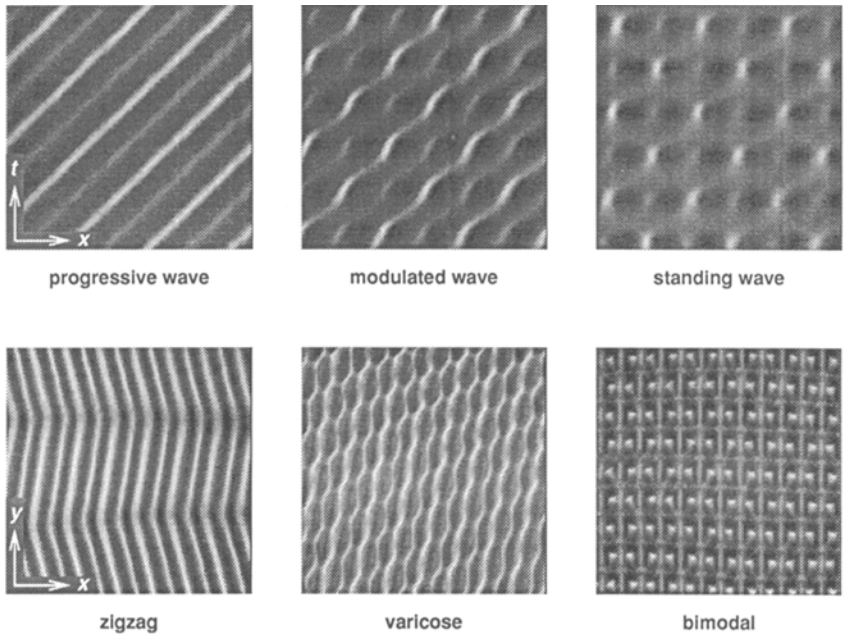

Fig. 4. Structures of the 1D nonlinear wave represented in the x, t space ($f = 95$ Hz, $V = 23.7$ V, $d = 15$ μm), and of the stationary states in the x, y space [$f = 45$ Hz, $d = 50$ μm, $V = 10.3$ V (zigzag), 11.2 V (varicose) 16.1 V (bimodal)].

e.g., the Varicose and Bimodal on one hand and the Modulated and the Standing Wave (SW) on the other hand (cf. Section 1.3). For instance, the SW is the superposition of two opposite progressive waves of equal amplitude. The experimental structures shown Fig. 4 reflect those symmetries. One expects then that the defects will have similar features in both states.

2.6. Defects in a 2D Space

A defect is a singularity of the order parameter which corresponds to a nonzero value of the total phase variation measured along any closed oriented contour encircling it: $\oint_c k\, ds = m \cdot 2\pi$. The condition for such a singularity to persist under any small perturbation is that the value of the integral is $m \cdot 2\pi$ (at least 2π). Then the defect is topologically stable. If the total phase variation over the portion of space where the structure is distorted is less than 2π, then the integral is zero, and the distortion does not correspond to a defect. Such a defect would be "unstable," i.e., cannot exist. Another case is when there is a phase jump of 2π, but transient. This case

is met, for instance, in a 1D space when the order parameter is a scalar. The topological stability is studied by representing each bifurcated state in the *order-parameter (OP) space.*[19]

There, the roll structure is represented by a circle Σ of radius A_0, parametrized by the phase $\varphi(x)$. Any closed contour C in the real space is mapped as a closed contour (a loop), its image C_1 in the OP space (Fig. 5). The topological stability of the defects is directly deduced from the properties of the relevant homotopy group of C_1 in the *order-parameter (OP) space.*[19] The defect is topologically unstable if the closed path on the contour C_1 in the OP space can be continuously deformed onto, i.e., can be homotopic to, a point. Many consequences result from these simple elements concerning the topological stability of defects, and hence their possible existence in the physical space.

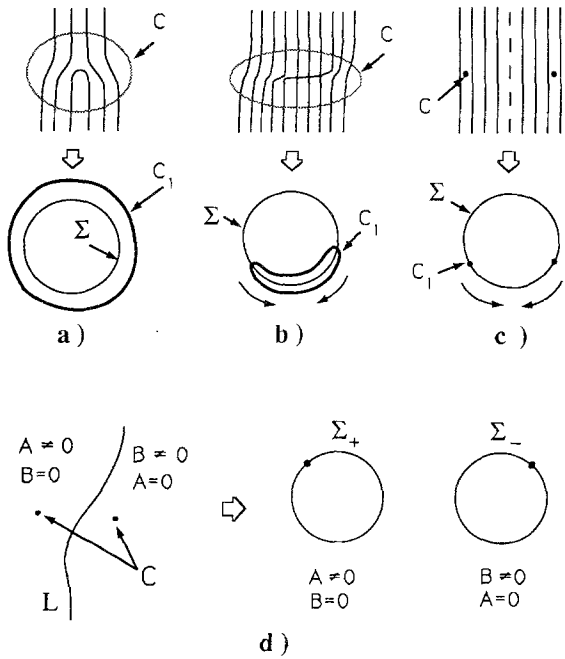

Fig. 5. (a) A closed contour C around a point defect and its image C_1 in the order-parameter space Σ. C_1 is not homotopic to a point and the defect is topologically stable. (b) The image of a contour C around a phase modulation where the phase variation is less than 2π is homotopic to a point. (c) The contour around a line defect in rolls with a 2π phase jump consists of two points on the circle Σ. This defect is unstable because the two points collapse. (d) The line defect is stable if there is a symmetry-parity breaking that leads to a set of disconnected circles in the OP space ("double state").

2.6.1. Point Defects in a 2D Space of Stationary Normal Rolls. They are codimension-2 defects. The codimension c is defined as $c = d_e - d_d$, where d_e is the dimension of the physical space and d_d the dimension of the defect.

The variation of order parameter is measured along a circle C (a sphere of dimension $r = c - 1$) around the defect P. If the total variation is 2π, the image of the contour in the OP space is also a closed loop C_1 around the OP circle Σ. Thus, it is not homotopic to a point. If the total phase variation is less than 2π, then the image of the closed contour cannot encircle Σ. The defect is not stable, but it can be observed as a transient state, as we shall see later. A defect corresponds to a singularity where the phase is undefined and it follows that a point defect is characterized by an amplitude $A_0 = 0$ at its core.

2.6.2. Line Defects in Normal Rolls. These defects of codimension $c = 1$ are defined by a contour of dimension $r = c - 1 = 0$, i.e., two points on both sides of the line. On the circle Σ the two points are also imaged by two points which can continuously get close together and collapse (Fig. 5). Thus, a line defect is not stable, and can be observed only as a transient.

2.6.3. Line Defects in a "Double State." In the stationary rolls the system is characterized by an invariance under any continuous translation along $\mathbf{y}$ or $-\mathbf{y}$. If this symmetry is broken, i.e., if, in real space, there can be two domains of states symmetrical with respect to some line along $\mathbf{y}$, then the line can be a stable defect. For instance, the Oblique Rolls structure is defined by a tilt $\pm\theta$ over $\mathbf{y}$. Thus, domains at θ are separated from domains at $-\theta$ by a defect which is named a *domain-wall* or a *grain boundary*, in analogy with defects in solids.[20]

The order parameter can be represented in each domain by

$$A_{\pm} \sim A_0(x) \exp i(k_x x \pm k_y y) \sim A_0(x) \exp i\varphi_{\pm}$$

The OP space is now composed of two disconnected circles $\Sigma_{\pm}$ each one parametrized by its own phase φ_+ or φ_- (Fig. 5). A contour enclosing a line defect will be represented by a set of two points each one on its respective circle. In this special situation the relevant homotopy group is the zeroth group, which indicates that, due to the nonconnectedness of the two circles, the defect is topologically stable.[19]

2.7. Defects in a 1D Space

There, the dimension of any defect reduces to zero, i.e., one has only point defects. The OP space for a periodic structure (a unique progressive

wave) is a circle Σ. The sphere enclosing the defect in the real space is composed of two points on both sides and its image is a set of two points on Σ that can always be reduced to one point. Then, any defect inside a progressive wave is unstable. But in fact, the solution consists of two counterpropagative waves and now the parity symmetry $\omega t \rightleftharpoons -\omega t$ is broken. The solution is

$$A_{\pm} \sim A_0(x) \exp i(k_x x \mp \omega t) \sim A_0(x) \exp i\varphi_{\pm}$$

The OP space is composed of two disconnected circles parametrized by the phases φ_+ and φ_-. In the real space a defect would consist of a point on x separating two opposite waves, and it will be stable because of the non-connectedness of the two circles.

If now one represents the waves in the 2D $\{x, t\}$ space, the point defect can be represented, although it is unstable (transient) in real space. It will appear as a dislocation. The second type of defect, which anyway persist stably,[17,24] will be represented as a *domain wall* separating domains of symmetrically tilted lines in a way quite similar to the *domain wall* in the stationary Oblique Rolls (Fig. 6).

In conclusion, it is the symmetry of the bifurcated state that defines the nature (the topography) of the defect and it is the class of homotopy groups in the order-parameter space that indicates its possible existence. However, the topological stability obviously cannot give any indication on

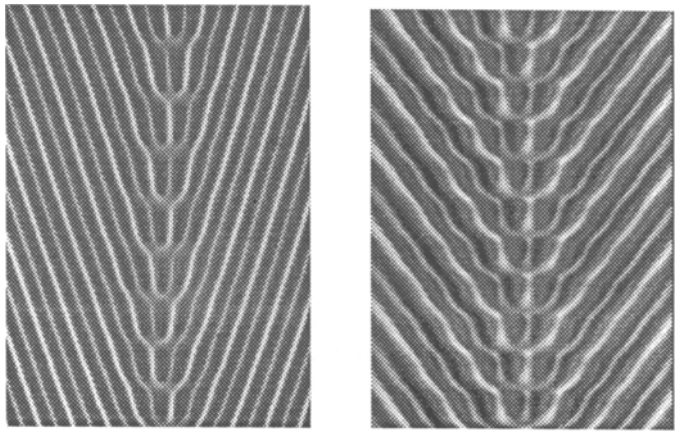

Fig. 6. Domain walls are line defects separating double states, (a) in the Oblique Rolls structure ($f = 45$ Hz, $V = 10.3$ V, $d = 50$ μm), (b) in progressive waves (here a source represented in the x, t space; $f = 95$ Hz, $V = 23.5$ V, $d = 15$ μm).

the creation process of defects, although it helps in understanding the dynamics of creation and annihilation of defects.

This geometrical analysis can be extended to other states, for instance, to the Bimodal state, which is here, too, equivalent to the standing-wave state of 1D nonlinear waves. In the following we shall describe the creation, the topology, and the instability of the defects first inside the stationary structures, and next inside the 1D nonlinear waves.

3. LOCALIZED INSTABILITIES AND DEFECTS IN THE STATIONARY ROLLS

3.1. Creation of Dislocations in the Normal Rolls

It was experimentally found that in the quasistationary Normal Rolls, one of the mechanisms of creation of dislocations consists of a localized instability of Varicose structure which occurs after a modulational instability takes place, triggered by a sudden and small increase of the voltage.[2] Once the voltage step $\Delta V/V \simeq 0.02$ is applied, a modulation of both the amplitude and the phase of some rolls occurs within some tenths of a second, in the **x** direction. Two rolls distant by about 1–4 wavelengths have a larger amplitude and a smaller diameter. This profile is constant along **y** and we name *walls* the larger amplitude rolls. Next, during a longer time, up to 100 sec, the local amplitude vanishes around one point centered inside the two *walls*. Simultaneously a localized modulation of the phase centered on this point pinches the few rolls between the *walls*. When the pinching reaches its maximum the rolls are cut along **x** into two parts which separate, forming then a pair of opposite dislocations. Therefore, the modulational instability *focuses the amplitude* around some point so that locally the pinching (Varicose) instability can be triggered with a value of the voltage that would be otherwise too low, by almost two orders of magnitude, to destabilize homogeneously the rolls.

3.2. Topology of Point Defects in Normal Rolls

A defect in the Normal Rolls structure corresponds to a phase jump of $\pm 2\pi$ on an oriented closed contour around its location.[6] In other words an extra period is added (or subtracted, depending on the sign + or −) in one of the two half-spaces defined by a line parallel to **x** passing through the defect center (Fig. 7).

A first indication of the velocity field inside the defect (the central part is named the *core*) is obtained by using interferometry in monochromatic parallel light.[5,9] In a homogeneous structure the molecular axis is tilted

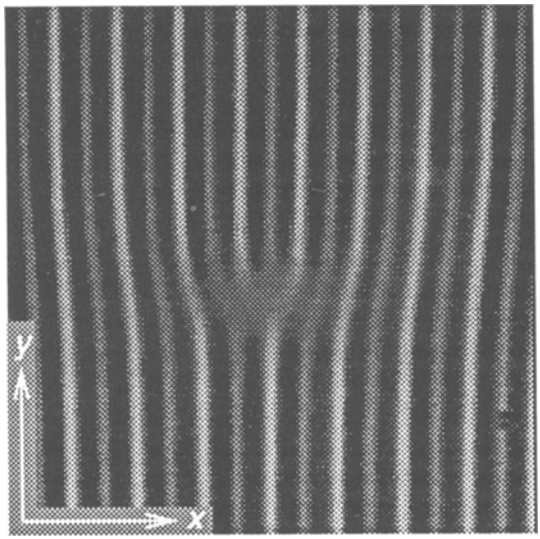

Fig. 7. An edge dislocation in Normal Rolls. In the upper half-plane an extra period is added. The core corresponds roughly to the undercontrasted central zone ($f = 60$ Hz, $V = 10.9$ V, $d = 50$ μm).

over **x** in the vertical plane with the periodicity of the convection, by an angle ψ which is a function of the velocity gradients. Then the index of refraction is modulated and birefringence measurements can give a direct access to the velocity gradients. Figure 8 shows the distribution of the isoclines (lines of equal tilt, i.e., of equal velocity gradient) in the rolls. The density of lines is higher close to the up and down flow lines and it vanishes to produce a singularity in the core of the defect. There, the tilt angle $\psi = 0$ and equal to that on the up and down lines.

By tracing glass spheres immersed in the fluid, one can represent the streamlines inside the core.[5,7,9] Inside a convective roll their motion is circular (i.e., contained in a vertical plane **xz**) when far from the defect. But when they are at a distance less than λ from the core there is an axial component which makes the trajectory helical. Close to the core, at a distance of order $\lambda/2$, the motion suddenly changes plane, and occurs for a short time in a plane almost normal to the previous one (Fig. 9). These motions clearly indicate the presence of stagnation points S which separate orthogonal streams taking place over a small volume of order a space period λ. Indeed, the same flow structure is found in the pinching of the varicose instability and also localized orthogonal rotations are the characteristics of the bimodal state.[6,8,9]

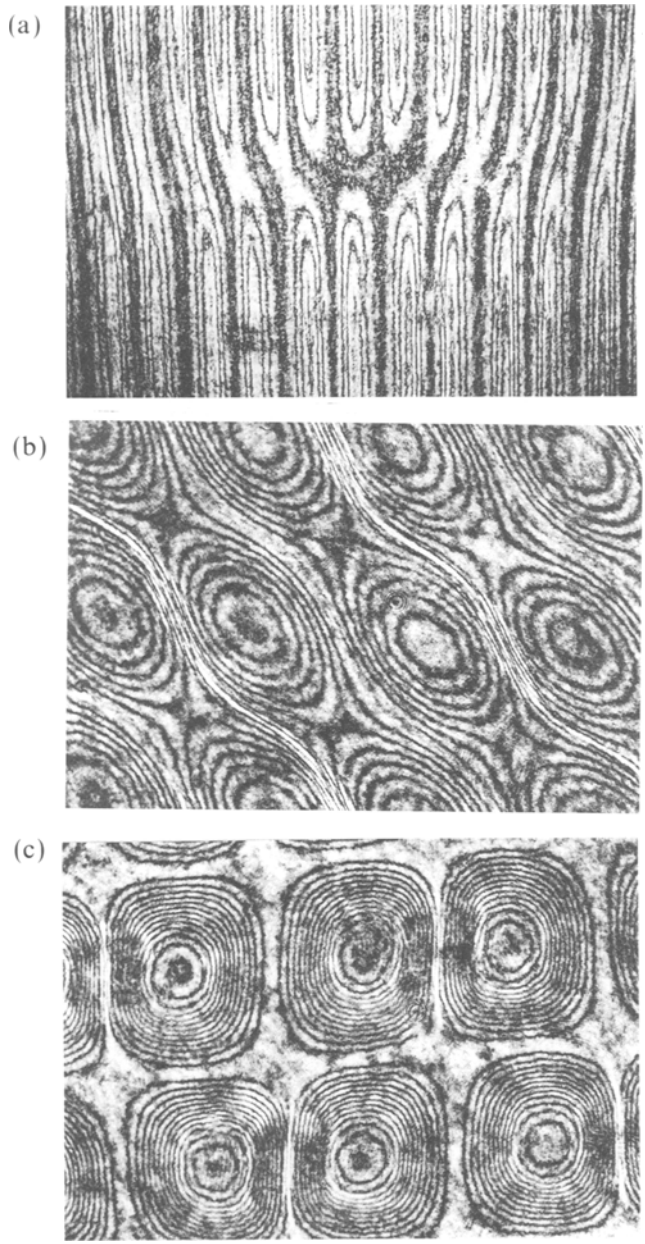

Fig. 8. Interference fringes showing the isoclines of constant velocity in (a) a dislocation, (b) a varicose, and (c) a bimodal structure. The higher the density of lines, the larger are the velocity gradients. In the pinched parts the velocity is lower.

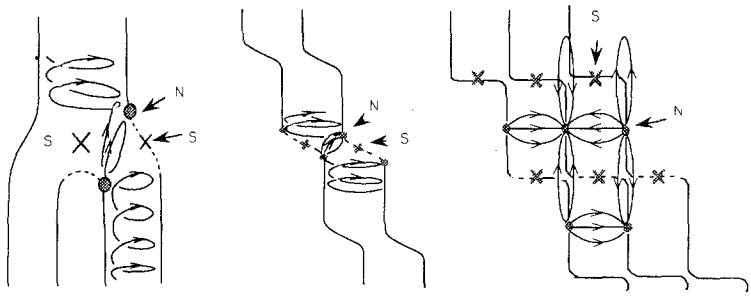

dislocation varicose bimodal

Fig. 9. Streamlines inside the dislocation, the varicose and the bimodal, as obtained from particle tracing. They show that a pinching produces stagnation points S and nodal points N and induces a rotation by $\pi/2$ of a flow element.

In conclusion, the core of the dislocation contains the symmetry elements of the state, which is stable only for higher values of the external stress. It is the topological constraint that forces the localized unstable state to appears as metastable. For instance, here, the core of the dislocation represents a Bimodal state, and in its vicinity the continuity with the Normal Rolls is made by a pinching of decreasing amplitude, i.e., by a damped Varicose structure.

Now if the core of a defect represents locally the unstable state inside a stable one, its stability under stress comes naturally as the problem of a local bifurcation to this yet unstable state. It will be shown hereafter that defects can mediate a transition to a homogeneous state whose symmetry is present in their core.

3.3. Instability of Point Defects in the Normal Rolls

Since the defect core is equivalent to a local unstable state, it can be made unstable by increasing the external stress. Experimentally, the voltage is smoothly applied and one observes a *dissociation*, i.e., an extension of the core width L_x. The core width is the length between points where the amplitude A takes an arbitrary value close to zero (e.g., 10% of the maximum of A). The initial value in the absence of extra stress is of order one roll diameter. The result shown in Fig. 10 indicates a threshold in the constraint beyond which the length L_x increases sharply. Also, the width L_y of the deformation field measured along y decreases to zero. The width L_y would be the analog of the width of a Bloch wall that connects two domains of opposite vorticity (at least around the core). This extension of L_x is analogous to the *core dissociation* in solids, where the dislocation

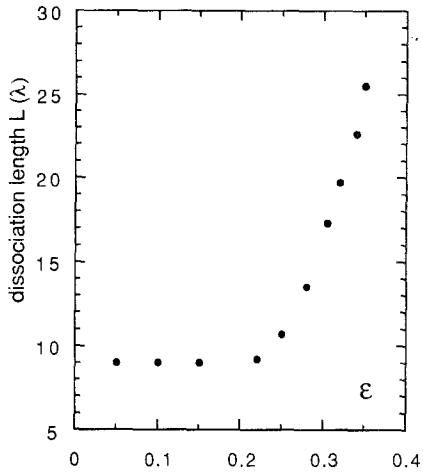

Fig. 10. Core stretching (dissociation) L_x under an increasing voltage measured by $\varepsilon = (V^2 - V_{th}^2)/V_{th}^2$.

splits into two halves (the "partials") which move apart along **x**.[20] In the part of the structure between the two partials the rolls are completely pinched, and on both sides of the *dissociation line* they are of opposite vorticity. The *dissociation line* is now a real singular line similar to an Ising wall. At this point the voltage is close to the threshold for the bimodal, and the topology of the dissociation line is precisely that of the singular lines parallel to **x** in the Bimodal. Increasing further the voltage, increases the density of such lines until they stack together at equal distances along **y**, thus forming domains of Bimodal structure, after a typical transient time. Figure 11 shows the rate of area transformed into a Bimodal after a sufficiently high step of voltage has been applied to reach the Bimodal threshold.

This rapid process involving the defects and geometrical transformations (shear, translations, and rotations) over distances larger than λ is quite similar to the so-called *displacive transitions* or Martensitic transformation in solids[21] subject to a fast temperature gradient, although, generally, displacive transitions imply first-order transitions (subcritical bifurcations).

3.4. Instability of Linear Defects in Normal Rolls

Line defects are topologically unstable. *Linear defects* are those which have the topology of point defects, but which are extended in one direction. So they are also codimension-2 defects. This is the case for the *dissociation*

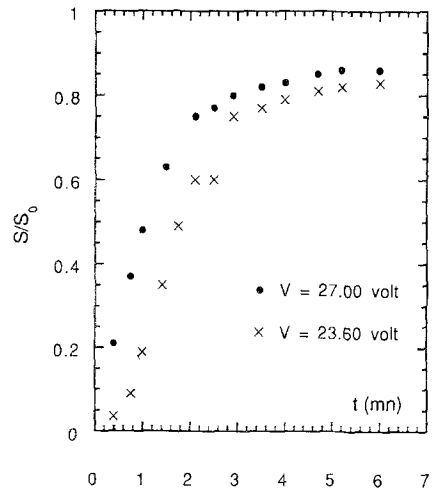

Fig. 11. Rate of area S of domain of Normal Rolls transformed into Bimodal as the time increases following the sudden application of a large voltage (S_0 is the total area of the sample).

lines, which, as we have just seen, are dislocations in which the core develops a bifurcation to a lower symmetry state, but where the phase jump is nevertheless 2π, as in a point defect.

Another case is when a localized modulation of the amplitude and of the phase in the form of a pinching extends on a line over a large distance without any apparent dislocation (Fig. 12). The geometry is close to that of a dissociated dislocation, but there is no defect. Such a localized perturbation is named a "*shear line*." It can be easily unstable under an external stress, giving birth to an even number (at least a pair) of opposite dislocations. In the same way a *dissociation line* may produce an odd number (at least three) of dislocations. In both cases the total topological "charge" is conserved. One has a dynamical process of creation and multiplication of defects, by dissociation of initial defects and relaxation of extended dissociated lines. The stress may also be internal, i.e., generated by the local field of heterogeneous modulations that characterize the complex state developed by a rapid application of the stress.

3.5. Regular Patterns of Defects

In some cases the modulational instabilities of the basic structure are periodic in space, giving rise to *supermodulated rolls*. Rolls equally spaced by a fixed number of periods $n\lambda$ (typically $n = 2, 3, 4$) have a larger amplitude and a smaller diameter. We call them "*walls*" (of discommen-

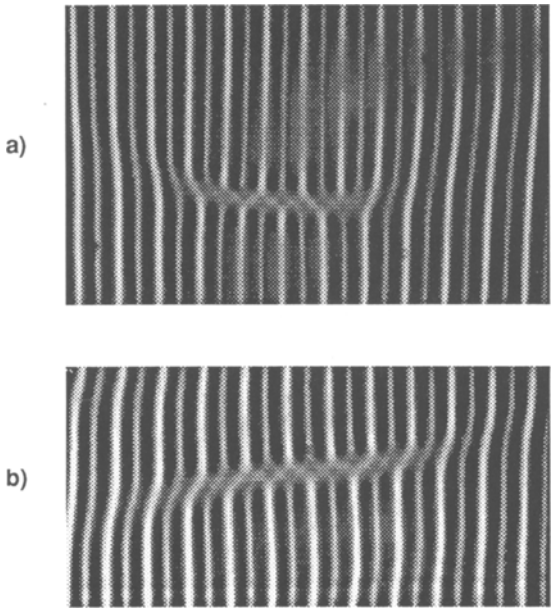

Fig. 12. (a) A dissociated core of a dislocation ($f = 70$ Hz, $V = 11.8$ V, $d = 50$ μm); (b) a "shear line" is a strong localized phase modulation, but not a defect. It can relax to give rise to a pair of dislocations ($f = 70$ Hz, $V = 11.8$ V, $d = 50$ μm).

suration). This case is commonly observed quite near the lowest frequency of the traveling-wave range. Then, as the voltage is increased *smoothly*, periodic distortions of shear occur in the space between the large-amplitude "walls" along **y** as in the nucleation process described in Section 2.1. However, the splitting does not occur here and the nucleation is aborted. One obtains a perfectly ordered state of periodic modulations of phase and amplitude (*walls*) along **x**, and periodic *shear lines* along **y** (Fig. 13). As the voltage is further increased, the *walls* disappear, the *shear lines* connect together in the **x** direction, and one recovers suddenly the Bimodal state since the *shear lines* have precisely the topology of the *dissociated lines* (or the basic singular lines of Bimodal).

3.6. Discussion

The core of stable defects has the symmetry elements of the unstable state. This state could therefore be "germinated" from the defects under a larger stress. However, one major question arises here. Such a transformation would imply in a classical picture of phase changes that the bifurca-

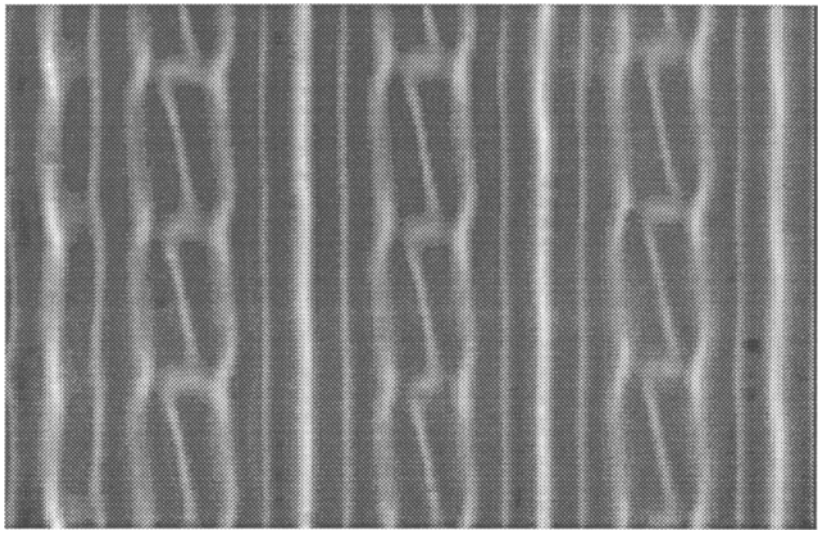

Fig. 13. Strong and localized modulations of rolls along the horizontal (x) and trapped dislocation pairs stacking along y give a regular array of localized bifurcated states ($f = 80$ Hz, $V = 12.0$ V, $d = 25$ μm).

tions be subcritical to allow the coexistence of domains with a different order parameter. But actual findings[5,25] indicate that the bifurcations are here supercritical.

4. LOCALIZED BIFURCATIONS IN NONLINEAR WAVES

4.1. Point Defects in Nonlinear Waves (Space-Time Dislocations)

In the $\{x, t\}$ space the point defect is here, too, a dislocation,[22] i.e., the sudden loss (or gain) at a given time of one space period (Fig. 14). It was shown that space-time dislocations occur after a localized perturbation of the phase.[22] Since here the phase is $\Phi = (kx - \omega t)$, a local modulation $\Phi(x)$ expresses a localized change in the velocity ($v = \omega/k$), i.e., a *shock*. In a shock, the local wavevector undergoes a sudden variation which pulls it beyond some stability limit (for instance, of the Eckhaus–Benjamin–Feir type). The restabilization occurs by expelling (in a compressive shock) or creating (in a dilative one) one spatial period. Then dislocations are created the charge of which is related to the type of shock.

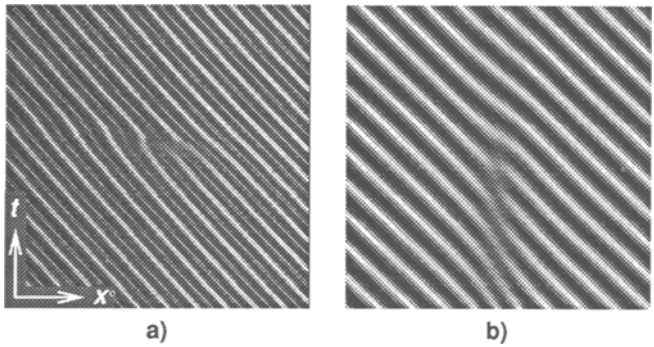

Fig. 14. (a) A space-time dislocation in a nonlinear 1D wave ($f = 105$ Hz, $V = 34.4$ V, $d = 10\ \mu$m) and (b) its numerical simulation with initial conditions $\alpha = 1$, $\beta = 0.4$, $\gamma = 1.4$, $\delta = c_g = 0$, $|A| = \text{const}$, $B = 0$, $\varphi_a = \pi\ \text{th}(x/4.4)$.

4.2. Pair of Dislocations

It is experimentally found that the creation of pair of dislocations is quite rare and the conditions for it are not yet clear. At the core of a dislocation the amplitude modulus $|A|$ vanishes and because of the coupling between left- and right-going waves (the two states are equally stable) any decrease in A, for instance, favors a correlative increase in B. By the numerical simulation of the coupled CLG equations, one verifies that dislocations are also solutions to the equations.[23] This is done by imposing as an initial condition a localized phase jump of 2π (Fig. 14).

4.3. Line Defects in Nonlinear Waves, Sinks, and Sources

They correspond to limits, the *domain walls*, separating two domains of counterpropagative waves, i.e., points (in 1D) where $|A| = |B|$ (Fig. 15). Those points are represented in the $\{x, t\}$ space as line defects.[24] A *domain wall* is a *sink* when the waves A and B meet at it and a *source* when they are emitted from it.

Sinks and sources are stable topological defects characterized by the coupling between the two states. At their core, $|A| = |B|$, which corresponds to the condition for a standing wave at *one point*.[22,23] Because of the competition between space gradients and nonlinearity, the amplitudes profile around this point is kinklike and over some finite distance there is a mixing of the two states. A mixing represents in fact a modulated wave (MW), the modulation amplitude decreasing with increasing distance from the wall. Figure 6b shows the modulated wave in the vicinity of a source. This structure is quite similar to that around the core of a dislocation. It is also identical to the structure of a *domain wall* in the

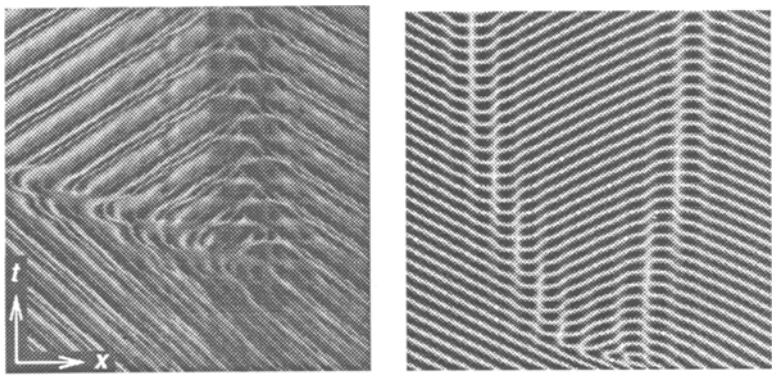

Fig. 15. The creation of a pair of domain walls, a source (left) and a sink (right). (a) Experiment ($f = 87$ Hz, $V = 28.1$ V, $d = 15$ μm); (b) simulation with same initial conditions as for the dislocation, except that now $|B| = 0.2\ \mathrm{sech}^4(4.4x)$.

Oblique Rolls structure because of the same symmetries.[5] The mechanism of creation of a pair sink-source is basically the same as for the creation of a pair of space-time dislocations, i.e., a compressive and a dilative shock. Numerically, the creation of a pair sink-source is achieved by imposing a local phase jump of 2π and simultaneously allowing a state B to grow from noise[23] (Fig. 15).

4.4. Instability of Sinks and Sources

The point defects are topologically unstable in the 1D physical space and therefore only the line defects which are topologically stable can be made unstable under stress. Here, too, it is the core structure that determines the unstable state of the defect. The core has the symmetry elements of a standing wave and is surrounded by a decreasing-amplitude modulated wave. It is then expected to be unstable against a localized standing wave at least transiently. Two typical cases are considered:

(a) Multiplication of sinks and sources.[23] Consider the case where the system is in the uniform wave state but close to the bifurcation to the standing wave. In the equations this comes to giving γ a value slightly higher than 1. In addition, one may allow phase fluctuations to occur, for instance, by satisfying the Benjamin–Feir criterion $1 + \alpha\beta < 0$. The result is the following: because the core represents the most unstable phase, any fluctuation will try to destabilize it. Then a standing-wave domain starts developing from the core. The finite lifetime of the phase instability makes

this state a transient and restabilization occurs either back to the initial defect or to an odd number of defects (to conserve the topological charge). In Fig. 16 a sink gives rise to a source plus two sinks. By numerical simulation of the coupled CLG equations one is able, following this scheme, to mimic the experimental multiplication of defects (Fig. 16a).

(b) Core-widening under stress.[25] The action of an appropriate external stress on a state of progressive waves makes them unstable to standing waves beyond some threshold. For instance, applying a modulation of the voltage at frequency 2ω, where ω is the frequency of the traveling wave, has for effect a coupling between the two A right- and B left-going waves.[26] In the equations this is done by adding a linear term in A or $\bar{B}$ to each CLG equation. As the depth of modulation increases, one passes continuously from the progressive wave PW to a modulated wave MW[27] and a standing wave SW.[30]

Let us start from a state of domains of progressive waves A and B separated by a *domain wall* (say a source). Applying an increasing external forcing makes the SW state in the core more and more stable inside the PW state, which in turn becomes more unstable. In space, this leads to an extension of the source width inside the unstable PW state. Experimentally, this variation is found to be nonlinear, diverging as the stable SW state is reached (Fig. 17). Such an instability is quite similar to the dissociation of dislocations described in Section 2.3. However, it is not expected from localized instabilities inside states that bifurcate supercritically. In effect, by analogy with the phase transitions in solids such a domain-wall widening is rather characteristic of subcritical bifurcations[28] (germination growth,

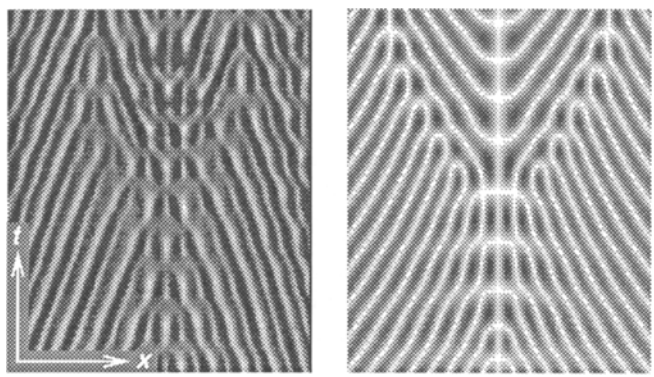

Fig. 16. A sink may become unstable and give rise to a source plus two sinks. (a) Experiment ($f = 95$ Hz, $V = 30$ V, $d = 10$ μm); (b) Simulation with $\alpha = 1$, $\beta = 0.4$, $\gamma = 1.02$, $\delta = c_g = 0$, $|A| = 0.5 \sin(2\pi x/100) + 0.5$, $B = -0.5 \cos(2\pi x/100) + 0.5$.

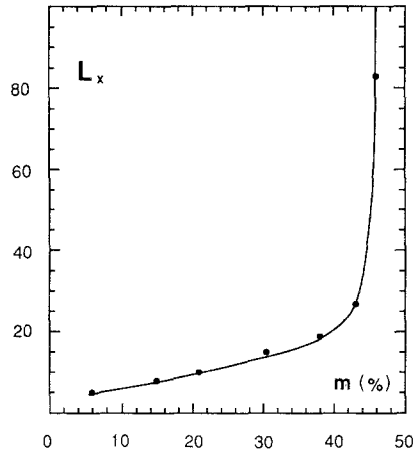

Fig. 17. Core stretching of a source under an increasing stress m (the coupling rate between left and right waves).

solidification fronts, transitions induced by grain boundaries). In fact, it has recently been shown that instability of space-time domain walls in the case of eventual subcritical bifurcations[29] would resemble the germination growth in solids.

We notice that both in the case of defects in stationary states or of defects in nonlinear waves the spatial extension of the local bifurcation has similar characteristics under stress (see Sections 3.3, 3.4).

5. CONCLUSION

It is found experimentally that either in stationary or time-dependent spatially uniform (homogeneous) states, local perturbations of the order parameter may induce singularities such as defects. The latter case is a novel phenomenon in nonlinear waves. The core of defects represents a local bifurcated state with a lower symmetry. Therefore the destabilization of the uniform state may start locally by the destabilization of the core of the defect. The instability of a defect may rise to several mechanisms that contribute either to the progressive disorganization of the basic state (defect multiplication) or to a bifurcation to a homogeneous state ("germination"). However, by analogy with phase transitions in solids, such a behavior, which would be expected when bifurcations are subcritical, raises a problem since the bifurcations are experimentally found to be supercritical. Nevertheless, most of the experimental effects concerning the creation, the structure, and the stability of defects can be reproduced numerically using these CLG equations. In the search for nonlinear

evolution equation starting from the basic microscopic equations of the nematoelectrohydrodynamics, one would certainly have to take into account the effects of localized bifurcations and instability of defects, without invoking subcritical bifurcations. Next, although not reported here, similar instabilities have been observed concerning the domain walls of the Oblique Roll structures, whereby the germination of the Bimodal can also be realized.

This study was motivated by the fact that usually the complex state is very commonly observed in between the first bifurcation, the Normal Rolls, and the last one, the Bimodal, before reaching chaos, instead of the secondary bifurcations, the Oblique Rolls and the Varicose. We understand now that this disordered state results from the application of a too large or a too fast stress increment; it involves local instabilities, creation of defects, and a time-dependent mode. It is similar to the so-called displacive transitions in solids, whereas the full sequence of bifurcations obtained only under the slow application of very small increments is the analog of a series of diffusive transitions.

ACKNOWLEDGMENTS

We acknowledge fruitful discussions with P. Coullet, J. Friedel, J. M. Ghidaglia, J. Lajzerowicz, L. Lega, and A. C. Newell. The numerical simulations on a CRAY2 computer were made possible by the Scientific Committee of the CCVR at Palaiseau. We are also grateful to F. Augier for valuable advice and help during the numerical simulations. This work has been performed under DRET contract 87/142.

REFERENCES

1. R. Krishnamurti, *J. Fluid. Mech.* **42**:295 (1970); J. P. Gollub, A. R. McCarriar, and J. F. Steinman, *J. Fluid. Mech.* **125**:259 (1982); E. Guazzelli, E. Guyon, and J. E. Wesfreid, *Phil. Mag. A* **48**:709 (1983).
2. X. D. Yang, A. Joets, and R. Ribotta, in *Propagation in Systems far from Equilibrium*, J. E. Wesfreid, H. R. Brand, P. Manneville, G. Albinet, and N. Boccara, eds. (Springer-Verlag, Berlin, 1988).
3. A. Joets and R. Ribotta, *Phys. Rev. Lett.* **60**:2164 (1988); also in *Propagation in Systems far from Equilibrium*; J. E. Westreid, H. R. Brand, P. Manneville, G. Albinet, and N. Boccara, eds. (Springer-Verlag, Berlin, 1988), p. 176; *Liquid Crystals* **5**:717 (1989).
4. E. Dubois-Violette, P. G. de Gennes, and O. Parodi, *J. Phys.* (Paris) **32**:305 (1971); P. G. de Gennes, *The Physics of Liquid Crystals* (Clarendon Press, Oxford, 1974).
5. A. Joets, Thesis, Paris VII (1984); R. Ribotta, in *Nonlinear Phenomena in Material Science*, L. Kubin and G. Martin, eds., Solid State Phenomena, Vol. 324 (Trans. Tech. Publications, Switzerland, 1988), p. 489.
6. A. Joets and R. Ribotta, *J. Phys.* (Paris) **47**:595 (1986).

7. A. Joets and R. Ribotta, *Europhys. Lett.* **10**:721 (1989).
8. A. Joets, X. D. Yang, and R. Ribotta, *Physica* **23D**:235 (1986).
9. R. Ribotta and A. Joets, *J. Phys.* (Paris) **47**:739 (1986).
10. F. H. Busse, *Rep. Prog. Phys.* **41**:1930 (1978); F. H. Busse and R. M. Clever, *J. Fluid. Mech.* **91**:319 (1979).
11. R. Ribotta, A. Joets, and L. Lei, *Phys. Rev. Lett.* **56**:1595 (1986).
12. S. Kai and K. Hirakawa, *Solid State Commun.* **18**:1573 (1976).
13. A. C. Newell and J. A. Whitehead, *J. Fluid. Mech.* **38**:279 (1969); L. A. Segel, *J. Fluid. Mech.* **38**:203 (1969); A. C. Newell, *Lect. Appl. Math.* **15**:157 (1974).
14. E. Bodenschatz, W. Zimmermann, and L. Kramer, *J. Phys.* (Paris) **49**:1975 (1988).
15. K. Kawasaki and T. Ohta, *Physica* **116A**:573 (1982); N. Bekki and K. Nozaki, *Phys. Lett. A* **110**:133 (1985).
16. G. B. Whitham, *Linear and Nonlinear Waves* (Wiley, New York, 1974); J. Lighthill, *Waves in Fluids* (Cambridge University Press, Cambridge, 1978).
17. P. Coullet, C. Elphick, L. Gil and J. Lega, *Phys. Rev. Lett.* **59**:884 (1987); P. Coullet and J. Lega, *Europhys. Lett.* **7**:511 (1988).
18. T. B. Benjamin and J. E. Feir, *J. Fluid. Mech.* **27**:417 (1967); J. T. Stuart and R. C. DiPrima, *Proc. R. Soc. Lond. A* **362**:27 (1978); C. S. Bretherton and E. A. Spiegel, *Phys. Lett.* **96A**:152 (1983).
19. G. Toulouse and M. Kléman, *J. Phys. Lett.* (Paris) **37**:149 (1976); N. D. Mermin, *Rev. Mod. Phys.* **51**:591 (1979).
20. J. Friedel, *Dislocations* (Pergamon Press, London, 1964); F. R. N. Nabarro, *Theory of Crystal Dislocations* (Clarendon Press, Oxford, 1969).
21. J. S. Bowles and J. K. Mackenzie, *Acta Met.* **2**:129, 224 (1954); J. W. Christian, *The Theory of Transformations in Metals and Alloys* (Pergamon Press, Oxford, 1965).
22. A. Joets and R. Ribotta, in *New Trends in Nonlinear Dynamics and Pattern Forming Phenomena: The Geometry of Nonequilibrium*, P. Coullet and P. Huerre, eds. (Plenum Press, New York, 1989); *J. Phys. C3* (Paris) **50**:171 (1989).
23. R. Ribotta and A. Joets, in *Partially Integrable Evolution Equations in Physics*, R. Conte and N. Boccara, eds. (Kluwer Academic, C-310, 1990), p. 279.
24. J. Lega, Thesis, Nice (1989).
25. A. Joets and R. Ribotta, preprint (1990).
26. D. Walgraef, *Europhys. Lett.* **7**:485 (1988).
27. E. Knobloch, *Phys. Rev. A* **34**:1538 (1986).
28. J. Lajzerowicz and J. J. Niez, in *Solitons in Condensed Matter Physics*, A. R. Bishop and T. Schneider, eds. (Springer, Berlin, 1978); *J. Phys. Lett.* (Paris) **40**:165 (1979).
29. P. Coullet, L. Gil, and D. Repaux, *Phys. Rev. Lett.* **62**:2957 (1989).
30. I. Rehberg, S. Rasenat, J. Fineberg, M. de la Torre Juarez, and V. Steinberg, *Phys. Rev. Lett.* **61**:2449 (1988).